

Nonlocal Surface-Wave Solitons

Barak Alfassi,¹ Carmel Rotschild,¹ Ofer Manela,¹ Mordechai Segev,¹ and Demetrios N. Christodoulides²

¹*Physics Department and Solid State Institute, Technion, Haifa 32000, Israel*

²*College of Optics/CREOL, University of Central Florida, Orlando, Florida 32816-2700, USA*

(Received 7 December 2006; published 21 May 2007)

We demonstrate, experimentally and theoretically, surface-wave solitons occurring at the interface between a dielectric medium (air) and a nonlinear material with a very long-range nonlocal response. These surface solitons are always attracted toward the surface, and unlike their Kerr-like counterparts, they do not exhibit a power threshold.

DOI: [10.1103/PhysRevLett.98.213901](https://doi.org/10.1103/PhysRevLett.98.213901)

PACS numbers: 42.65.Tg

Surface waves, localized waves propagating at the interface between two media with different optical properties, are among the most intriguing phenomena in optics. Surface waves display unique features having no analogues in homogeneous media, which make them useful for exploring the properties of material interfaces [1–3]. In the linear optical domain, a TM polarized surface wave can exist at the interfaces between metal and dielectrics [2], between a periodic layered system and a homogeneous medium [4], or between anisotropic and isotropic materials [5,6]. In addition to linear surface states, optical surface waves can also arise from nonlinearity [7], at the interface between two media of which at least one of them is nonlinear. The properties of nonlinear (Kerr) surface waves have been analyzed theoretically [8–12], revealing a power threshold for their existence. Interestingly, such threshold behavior has only recently been observed at the interface of nonlinear waveguide arrays [13–15]. Another type of nonlinearity supporting surface waves occurs in photorefractives driven by carrier diffusion [16,17]. However, thus far all studies on nonlinear surface waves have only considered local nonlinearities, such as Kerr [8–11] and the photorefractive diffusion nonlinearity [16,17], which is effectively local for beams much wider than the Debye length [18].

An important class of nonlinear material systems is those exhibiting nonlocal nonlinearities [19]. Such nonlinearities arise in several branches of physics, ranging from Bose-Einstein condensates to plasmas. In nonlinear optics, nonlocality can be encountered, for example, in liquid crystals [20,21] and in thermal nonlinear media [22,23]. As demonstrated recently [23,24], nonlocality can lead to new families of waves that would have been otherwise impossible in local, isotropic, nonlinear media. In view of this novel behavior, one may naturally ask whether surface solitons are possible under nonlocal conditions. And if they are, how do they differ from surface-wave solitons in local nonlinear media?

Here, we present the first study of nonlocal surface-wave solitons: self-trapped beams propagating at the interface between air and a nonlocal nonlinear medium. Both TE and TM polarized nonlinear surface waves are investigated. We show that nonlocal surface solitons are funda-

mentally distinct from their local counterparts. One difference that sets them apart is the fact that they do not exhibit a power threshold (unlike Kerr-like surface solitons). Another fundamental feature is that they reside mostly in the medium of higher index, which is also nonlinear, and they are attracted to the surface, even from very far away (exceeding the beam width by orders of magnitude), whereas in local nonlinearities a surface soliton must be launched at the vicinity of the interface, on the side of the lower-index medium [8]. The attraction to the surface leads to oscillations about the soliton (“equilibrium”) position.

As an archetypical system for long-range nonlocal nonlinear interactions, we use the thermal optical nonlinearity, which occurs in lead glasses [22]. In this medium, an increase in the optical intensity results in a temperature change, ΔT , and consequently to a proportional increase in the refractive index $\Delta n = \beta \Delta T = \beta(T - T_0)$, where T_0 is the temperature in the absence of light, and $\beta = dn/dT$ is the thermal coefficient of the refractive index. In lead glass, $\beta > 0$; thus, the nonlinearity is of the self-focusing type. The light beam gets slightly absorbed and heats the glass, thus acting as a heat source. Under steady state conditions, ΔT , induced by the intensity of the light beam $I(x, y, z)$, satisfies the heat diffusion equation [23,25]

$$\kappa \nabla^2 T(x, y, z) = -\alpha I(x, y, z), \quad (1)$$

where κ is the thermal conductivity of lead glass and α is the absorption coefficient. We are naturally interested in surface waves that are much narrower than the width of the sample, and are bound to a single interface.

Consider first the simple case sketched in Fig. 1(a), where the wave is narrow in x , uniform in y , and propagating along z . Here, the width of the sample is $2d$, and the interface at $x = d$ is between the nonlocal nonlinear medium with a refractive index n_1 (in the absence of light), and a linear medium of refractive index n_2 ($< n_1$). The nonlinear index change, Δn , is proportional to ΔT determined from Eq. (1). We take the thermal conductivity of the linear medium to be much smaller than κ ; hence, we can safely assume that the interface at $x = d$ is thermally insulating, thus posing the boundary condition

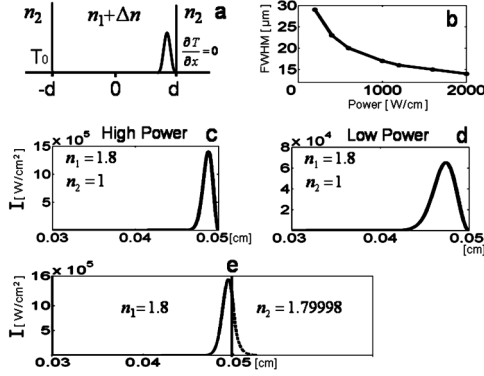


FIG. 1. (a) Sketch of a 1D surface soliton with its boundary conditions for the temperature. (b) Calculated width (FWHM) of a 1D surface soliton as a function of the 1D optical power density. (c),(d) Profile of a 1D surface soliton at high and low optical power, respectively. (e) 1D surface soliton for $n_1 - n_2 = 2 \times 10^{-5}$; the low index contrast at the boundary supports surface solitons with a significant part of their optical power residing in the linear medium.

$\partial T(x = d, y, z) / \partial x = 0$ for all y and z . The other boundaries of the sample are all connected to a heat sink held at temperature T_0 ; thus, the additional boundary conditions are $T(x = -d, y, z) = T(x, y = \pm d, z) = T_0$. The boundary conditions associated with Eq. (1) directly affect the temperature distribution in the sample, hence affecting the index change Δn induced by the optical intensity I .

To identify surface solitons, we express the optical field as $\vec{E}(x, y, z, t) = \vec{E}(x, y)e^{i(\Gamma z - \omega t)}$, ω being the frequency. Substituting the field in the Helmholtz equation yields

$$\nabla_{\perp}^2 \vec{E}(x, y) + [k_0^2(n_1^2 + 2n_1\Delta n) - \Gamma^2]\vec{E}(x, y) = 0, \quad (2a)$$

in the nonlinear medium (i.e., for $|x| \leq d$), where $|\Delta n| \ll n_1$, and

$$\nabla_{\perp}^2 \vec{E}(x, y) + [k_0^2 n_2^2 - \Gamma^2]\vec{E}(x, y) = 0 \quad (2b)$$

in the linear medium ($x \geq d$), $k_0 = \omega/c$, and $\nabla_{\perp}^2 = \partial_x^2 + \partial_y^2$. We express the field in the different media as $\vec{E}(x \leq d, y) = \vec{A}(x, y)$ and $\vec{E}(x \geq d, y) = \vec{B}(x, y)$. Δn in medium 1 depends on $I = |A|^2$, through Eq. (1) and the relation between ΔT and Δn . The boundary conditions for the fields at the interface depend on the polarization. For TE polarization ($\vec{A} = A\hat{y}$), the continuity of the transverse field and its derivative implies $A(x = d, y) = B(x = d, y)$ and $\partial_x A(x = d, y) = \partial_x B(x = d, y)$. The boundary conditions for the TM polarization can be expressed in a similar fashion on the magnetic field. At the other transverse interface (at $x = -d$), we assume that \vec{A}, \vec{B} and their derivatives vanish; i.e., the width of the surface solitons is much smaller than the sample width, $2d$. Note, that because the problem is nonlinear, the propagation constant Γ depends on the optical power, in contrast to linear surface waves where Γ depends only on the wave numbers in both media.

We first find numerically (1 + 1)D surface soliton in the configuration sketched in Fig. 1(a). The parameters for the simulation were taken from the experimental parameters:

$2d = 0.1$ cm, $\alpha = 0.01$ [cm⁻¹], $T_0 = 25$ [°C], $\kappa = 0.00637$ [W K⁻¹ cm⁻¹], $\beta = 1.4 \times 10^{-5}$ [K⁻¹]. To find a 1D surface self-trapped wave, we solve Eqs. (1), (2a), and (2b) self-consistently [23], with the boundary conditions described above. The solution is a surface-wave soliton, localized in the nonlinear material at the proximity of the boundary. Typical examples for the case of a boundary between lead-glass material ($n_1 \cong 1.8$) and air ($n_2 = 1$) are shown in Figs. 1(c) and 1(d), for high and low 1D optical power density, $P = 2000$ and 200 W/cm, respectively. The example of Fig. 1(d) corresponds to a ~ 40 μm FWHM surface soliton, with parameters close to those used in the experiment. The large refractive index difference between the lead glass and air ($n_1 - n_2 \cong 0.8$), and the continuity of the electric field at the boundary, imply that the soliton resides almost fully inside the lead-glass material, with only an evanescent tail in the air region. For the same reason, the wave functions of the TE and TM solitons are practically identical (at the same optical power) and share the same qualities. It is, however, important to note that such nonlocal surface solitons can be found at *any* optical power level, and hence there is no threshold for their formation. To exemplify that, Fig. 1(b) shows the width of the soliton as a function of optical power (for power levels that can still support solitons much narrower than the sample width, as we assume). As the optical power decreases, the soliton becomes wider and its peak is located farther away from the boundary [Fig. 1(d)]. Interestingly, when the boundary is between two media with a small refractive index difference, $n_1 - n_2$, such that it is comparable to the nonlinear index change ($\Delta n \approx 2 \times 10^{-5}$ under our experimental parameters), the boundary condition on the electric field allows surface solitons with a significant part of their optical power residing in the linear medium [Fig. 1(e)].

Next we find (2 + 1)D surface-wave solitons, residing at a planar interface, in the configuration sketched in Fig. 2(a). The solutions are found in a fashion similar to the (1 + 1)D case, under the same boundary conditions. Typical solutions are shown in Figs. 2(b) and 2(c), for optical power $P = 1.6$ W, $\lambda = 488$ nm, where $n_1 = 1.8$, $n_2 = 1$ (air) in Fig. 2(b), and $n_1 = 1.8$, $n_2 = 1.79998$ in Fig. 2(c) (with the other parameters as in the 1D case). As in 1D, there is no threshold for the formation of a 2D surface soliton. Likewise, the dependence of the soliton width on the optical power P has a trend similar to the 1D case. The 2D surface solitons have their peak (maximum intensity) shifted from the interface, with the shift depending on the index difference $\Delta \equiv n_1 - n_2$: the larger Δ is, the less the surface wave penetrates into the lower-index medium.

Having demonstrated the existence of 1D and 2D surface solitons in the nonlocal nonlinear medium, we proceed to study their robustness. We first test for stability by simulating their dynamics in the presence of noise. The example shown in Fig. 3(a) depicts the propagation of a surface soliton (located at $x = x_0$) for a distance of 30 cm

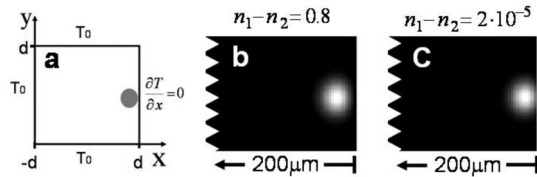


FIG. 2. (a) Sketch of a 2D surface soliton, with its boundary conditions for the temperature. (b) 2D surface soliton for $n_1 - n_2 = 0.8$. (c) 2D surface soliton for $n_1 - n_2 = 2 \times 10^{-5}$.

(~ 15 diffraction lengths), launched in the presence of 5% random noise (amplitude and phase). As shown in Fig. 3(a), the soliton is very stable, propagating smoothly without distortion or deviations in its trajectory. Keeping in mind the nonlocal properties of the medium, the straight line trajectory of this soliton manifests the fact that a surface soliton in a nonlocal medium forms when the force exerted on the beam by the nearby interface is equal to the force exerted by the distant boundary to the left (at $x = -d$). This understanding becomes even more significant when a narrow beam, of sufficiently high power to form a soliton, is launched away from the position of surface soliton (but still at a reasonable proximity to the interface). Figure 3(b) shows such an example, where we simulate the propagation of the same beam as in Fig. 3(a), but launched $30 \mu\text{m}$ away from the center point of the surface soliton [of Fig. 3(a)]. The beam in Fig. 3(b) maintains a localized shape, but it is pushed toward the interface and undergoes total internal reflection from it. The beam then moves past the center point of the surface soliton expected under such launch parameters, but is again attracted to the surface, where it bounces from the surface again, in a fully periodic fashion. The oscillations are periodic, and the beam never converges to a soliton of a straight line trajectory. This is perhaps one of the most interesting features of surface solitons in nonlocal nonlinearities: a beam launched away from the surface moves to the interface and “sticks” to its vicinity, even if the launch position is far away from the position of the surface soliton [26].

It is possible to understand the dynamics of a narrow beam launched away from the interface, by analyzing the forces exerted on it by the boundaries. For example, consider the “force” exerted on a 1D beam of intensity $I(x)$ and 1D power density $P = 200 \text{ W/cm}$, launched at a distance much larger than the distance of the correspond-

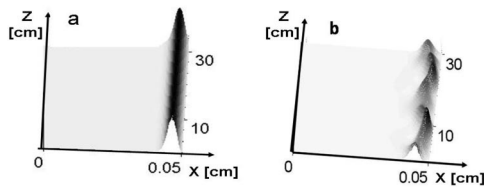


FIG. 3. Simulated propagation of (a) a surface soliton launched at its stationary position (x_0) with 5% noise, and (b) a beam of the same power launched $30 \mu\text{m}$ away from the stationary position. In the latter case, the beam forms a soliton oscillating about the stationary position.

ing surface soliton from the interface [Fig. 4(a)]. The diffusion of the heat generated by the (small) absorption of the beam creates the temperature profile denoted as $T_{1D}(x)$ in Fig. 4(a). As shown there, in the 1D case the temperature is constant between the peak of the beam (x_1 , center launch point) and the interface, i.e., for $x_1 \leq x \leq d$, whereas for $x < x_1$ the temperature is decreasing monotonically. That is, in (1 + 1)D, because the interface is thermally insulating, the temperature at the surface is identical to the temperature at the launch point (center of the input beam). This temperature distribution, translated into Δn , implies a net force [proportional to $\bar{\nabla}n/n = \bar{\nabla}(\Delta n)/n$ via the Eikonal equation] is pushing the beam toward the insulating surface. The surface soliton forms when the $\bar{\nabla}n/n$ force is balanced by a “surface force” (arising from $n_1 - n_2$) exerted on the beam by the interface. The 2D case reveals similar findings. Consider a 2D beam of power $P = 1.6 \text{ W}$ launched at $(x_1, 0)$, also shown in Fig. 4(a). In this 2D case, the cross sections (in the x direction) of the temperature profile, designated by $T_{2D}(x, y = 0)$ in Fig. 4(a), reveal that both boundaries exert forces on the beam, but the forces are unequal, resulting in a net force pushing the beam toward the insulating interface. In the y direction, when both top and bottom boundaries are maintained at an equal temperature, the net force is central, resulting in oscillation about $y = 0$ [27]. If the 2D beam is launched in the $y = 0$ plane, the motion of the beam is restricted to that plane [Fig. 4(b)].

To summarize the understanding, in both 1D and 2D, a narrow beam of sufficiently high power launched away from the launch point of the respective soliton ($x_1 \neq x_0$, $y = 0$) is attracted to the insulating interface, and bounces from the interface repeatedly, oscillating about x_0 , $y = 0$. Because the top and bottom boundaries are kept at a fixed temperature T_0 , they cannot support surface waves. Moreover, in the configuration of Fig. 2(a), simple (singly humped) surface solitons can form only at $y = 0$, where the forces exerted by the top and bottom boundaries cancel each other. Hence, any high-power, narrow, 2D beam launched at $y \neq 0$ oscillates about $y = 0$.

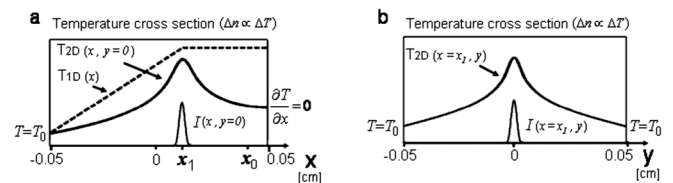


FIG. 4. The temperature profile induced by a surface soliton launched at $(x_1 \neq x_0, y = 0)$ ($x_0, 0$ being the center point of the surface soliton under the respective parameters). (a) The asymmetric cross sections of the temperature profile, taken in the x direction, for a 1D soliton [marked by $T_{1D}(x)$], and for a 2D soliton $T_{2D}(x, y = 0)$. In both cases, there is a net force pushing the beam toward the insulating interface at $x = d = 0.05$. (b) The symmetric cross section (taken in the y direction) of the temperature profile induced by the 2D soliton launched at $(x_1, 0)$.

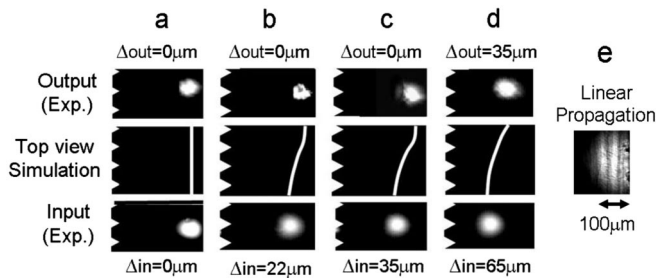


FIG. 5. Experimental photographs taken at the input and output faces of the sample, along with the respective calculated trajectories (top view) of the soliton. (a) A 2D surface soliton launched at its stationary position $(x_0, 0)$. (b),(c) A 2D surface soliton launched 22 and 35 μm to the left of $(x_0, 0)$. All the trajectories of (a)–(c) converge to the same output position, and the beams emerge as a surface soliton, at the close proximity of the insulating interface. (d) A 2D soliton launched 65 μm to the left of $(x_0, 0)$ moves toward the interface, but cannot converge to the proximity of $(x_0, 0)$ within the finite propagation length in our sample. (e) At low power, the input beam of (a) broadens considerably, and its intensity is modulated by interference with reflections from the interface, as shown in (e).

We now describe our experiments, all carried out in $(2 + 1)$ D settings. We launch a TE polarized Gaussian beam of 50 μm FWHM into a lead-glass sample of dimensions $2 \times 2 \times 80 \text{ mm}^3$. We set the boundary temperatures as explained above, and launch the beam at the expected location of the surface soliton, $\sim 30 \mu\text{m}$ away from the air-glass interface [Fig. 5(a), bottom panel]. The beam forms a surface soliton at $P = 1.2 \text{ W}$, exiting the sample at the same position relative to the interface [Fig. 5(a), top panel]. [For comparison, at low power the beam broadens to $\sim 200 \mu\text{m}$ [Fig. 5(e)].] Between the input and output experimental data, we add a top view of a simulation result of the soliton trajectory, which facilitates a comparison between theory and experiment. To demonstrate that this is indeed a surface wave, we move the launch point of the input beam by another 22 μm [Fig. 5(b)] and 35 μm [Fig. 5(c)] from the center point of the surface soliton [of Fig. 5(a)], while keeping the launch trajectory parallel to the z axis. The output beam observed in these experiments is shown in the top panels of Figs. 5(b) and 5(c), respectively. In both cases, the input beam moves to the interface, and sticks to its vicinity, exiting the medium at the same position as the ideally launched surface soliton [of Fig. 5(a)]. [The period of the oscillations calculated in Fig. 3(b) is too large to be observed in our 83-mm-long samples]. However, when the launch point of the input beam is moved too far away (65 μm) from the center point of the surface soliton [Fig. 5(d), bottom], the dynamics is different: the soliton still moves toward the interface, but the propagation distance (83 mm) is too short to allow convergence to the position of an ideally launched surface soliton. Consequently, the beam emerges at a distance considerably away from the insulating boundary [Fig. 5(d), top panel]. This result is corroborated by our

simulations. Finally, we repeat all of these experiments for a TM polarized beam and obtain the same results, as expected and as explained above.

To conclude, we presented the first studies of nonlocal surface-wave solitons. We find that narrow optical beams propagating in nonlocal nonlinear media display very strong attraction to the surface, even when launched from far away. This feature is unique to nonlocal nonlinearities, and offers a means to manipulate optical beams that follow adiabatically bent interfaces, along which surface-wave solitons can “flow.”

This research was supported by the Israel-U.S.A. Binational Science Foundation and by the Israeli Science Foundation.

-
- [1] A. Zangwill, *Physics at Surfaces* (Cambridge University Press, Cambridge, New York, 1998).
 - [2] W.L. Barnes, A. Dereux, and T.W. Ebbesen, *Nature* (London) **424**, 824 (2003).
 - [3] E. Altewischer *et al.*, *Nature* (London) **418**, 304 (2002).
 - [4] P. Yeh, A. Yariv, and A. Y. Cho, *Appl. Phys. Lett.* **32**, 104 (1978).
 - [5] D. Artigas and L. Torner, *Phys. Rev. Lett.* **94**, 013901 (2005).
 - [6] L. C. Crasovan *et al.*, *Opt. Lett.* **30**, 3075 (2005).
 - [7] A.D. Boardman *et al.*, in *Nonlinear Surface Electromagnetic Phenomena*, edited by H. E. Ponath and G. I. Stegeman (North-Holland, Amsterdam, 1991), p. 73.
 - [8] W. J. Tomlinson, *Opt. Lett.* **5**, 323 (1980).
 - [9] N. N. Akhmediev *et al.*, *Sov. Phys. JETP* **61**, 62 (1985).
 - [10] C. T. Seaton *et al.*, *IEEE J. Quantum Electron.* **21**, 774 (1985).
 - [11] K. Ogusu, *Opt. Lett.* **16**, 312 (1991).
 - [12] D. Mihalache, M. Bertolotti, and C. Sibilia, *Prog. Opt.* **27**, 229 (1989).
 - [13] K. G. Makris *et al.*, *Opt. Lett.* **30**, 2466 (2005).
 - [14] S. Suntsov *et al.*, *Phys. Rev. Lett.* **96**, 063901 (2006).
 - [15] Y. V. Kartashov *et al.*, *Phys. Rev. Lett.* **96**, 073901 (2006).
 - [16] G. S. Garcia Quirino *et al.*, *Phys. Rev. A* **51**, 1571 (1995); *J. Opt. Soc. Am. B* **13**, 2530 (1996); V. A. Aleshkevich *et al.*, *Phys. Rev. E* **64**, 056610 (2001).
 - [17] M. Cronin-Golomb, *Opt. Lett.* **20**, 2075 (1995).
 - [18] M. Segev *et al.*, *Phys. Rev. Lett.* **73**, 3211 (1994); D. N. Christodoulides and M. I. Carvalho, *J. Opt. Soc. Am. B* **12**, 1628 (1995); M. Segev, M. Shih, and G. C. Valley, *J. Opt. Soc. Am. B* **13**, 706 (1996).
 - [19] O. Bang *et al.*, *Phys. Rev. E* **66**, 046619 (2002).
 - [20] J. F. Heninot *et al.*, *Mol. Cryst. Liq. Cryst. Sci. Technol., Sect. A* **375**, 631 (2002).
 - [21] M. Peccianti *et al.*, *Appl. Phys. Lett.* **81**, 3335 (2002).
 - [22] F. W. Dabby and J. R. Whinnery, *Appl. Phys. Lett.* **13**, 284 (1968).
 - [23] C. Rotschild *et al.*, *Phys. Rev. Lett.* **95**, 213904 (2005); *Nature Phys.* **2**, 769 (2006).
 - [24] C. Rotschild *et al.*, *Opt. Lett.* **31**, 3312 (2006).
 - [25] M. D. Iturbe-Castillo *et al.*, *Opt. Lett.* **21**, 1622 (1996).
 - [26] Self-bouncing was also predicted to occur in the photorefractive diffusion-type nonlinearity by D. N. Christodoulides and T. H. Coskun, *Opt. Lett.* **21**, 1220 (1996).
 - [27] B. Alfassi *et al.*, *Opt. Lett.* **32**, 154 (2007).